Heliyon 10 (2024) e39309

Contents lists available at ScienceDirect

Heliyon

journal homepage: www.cell.com/heliyon

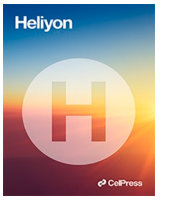

Research article

Spatiotemporal variation and GeoDetector analysis of NDVI at the northern foothills of the Yinshan Mountains in Inner Mongolia over the past 40 years

Bo Yao [a,b,c,d], Xiangwen Gong [b,c,d,**], Yulin Li [b,c,d], Yuqiang Li [b,c,d], Jie Lian [b,c,d], Xuyang Wang [b,c,d,*]

[a] Yinshanbeilu Grassland Eco-hydrology National Observation and Research Station, China Institute of Water Resources and Hydropower Research, Beijing, 100038, China
[b] Northwest Institute of Eco-Environment and Resources, Chinese Academy of Sciences, Lanzhou, 730000, China
[c] University of Chinese Academy of Sciences, Beijing, 100049, China
[d] Naiman Desertification Research Station, Northwest Institute of Eco-Environment and Resources, Chinese Academy of Sciences, Tongliao, 028300, China

ARTICLE INFO

Keywords:
NDVI
Spatiotemporal variation
GeoDetector
Climatic factors
Inner Mongolia

ABSTRACT

The study of spatiotemporal variation and driving forces of the normalized difference vegetation index (NDVI) is conducive to regional ecosystem protection and natural resource management. Based on the 1982–2022 GIMMS NDVI data and 26 influencing variables, by using the Theil-Sen median slope analysis, Mann-Kendall (M − K) test method and GeoDetector model, we analyzed the spatial and temporal characteristics of vegetation cover and the driving factors of its spatial differentiation in the northern foothills of the Yinshan Mountains in Inner Mongolia. The NDVI showed a significantly increasing trend during 1982–2022, with a growth rate of 0.0091 per decade. It is further predicted that future change in NDVI will continue the 1982–2022 trend, and sustainable improvement will dominate in the future; however, 17.69 % of vegetation will degrade, that is, NDVI will degrade instead of improvement. The spatial distribution of the NDVI in the northern foothills of the study area was generally characterized by high in the east and low in the west. Annual precipitation (Pre), evapotranspiration (Evp), relative humidity (Rhu) and sunshine hours (Ssd) had >70 % explanatory power (73.5, 79.9, 79.0, and 74.9 %, respectively). The explanatory power of edaphic factors was >30 %, whereas anthropogenic and topographic factors had little influence on the spatial variation of NDVI, with an explanatory power of <30 %. Thus, climatic factors were the dominant factors influencing the spatial variability of NDVI in the study area. The results of the interaction detector analysis showed nonlinear strengthening for any two factors, and the interaction between Rhu and barometric pressure had the highest explanatory power. There were optimal ranges or characteristics of each factor that promoted vegetation growth. This study investigated the differences in the explanatory power of different

* Corresponding author. Northwest Institute of Eco-Environment and Resources, Chinese Academy of Sciences, 320 Donggang West Road, Lanzhou, 730000, China.
** Corresponding author. Northwest Institute of Eco-Environment and Resources, Chinese Academy of Sciences, 320 Donggang West Road, Lanzhou, 730000, China.
E-mail addresses: gongxiangwen@nieer.ac.cn (X. Gong), xuyangwang@lzb.ac.cn (X. Wang).

https://doi.org/10.1016/j.heliyon.2024.e39309
Received 1 March 2024; Received in revised form 6 October 2024; Accepted 11 October 2024
Available online 12 October 2024

factors on the NDVI and the optimal range of individual factors to promote vegetation growth, which can provide a basis for the development of vegetation resource management programs.

1. Introduction

Global warming has led to an increase in the frequency of extreme weather and climatic events with significant impacts on ecosystems [1]. Vegetation is an important component of terrestrial ecosystems, connecting multiple cycles such as the atmosphere, land cycles, and hydrosphere [2], and plays a crucial role in ecosystem services such as soil and water conservation, climate regulation, and carbon and nitrogen cycling [3]. Therefore, it is important to study changes in vegetation and their driving forces in the ecological environment.

The study of vegetation change has attracted much attention, and the normalized difference vegetation index (NDVI) is an indicator that can better reflect the overall growth status of vegetation, which shows a good linear relationship with vegetation cover [4], and has been widely used to monitor the spatial and temporal dynamics of vegetation [5–8]. Differences in hydrothermal conditions across regions can significantly affect vegetation growth in terrestrial ecosystems [9], and precipitation (Pre) is a key factor controlling vegetation growth, particular in arid and semi-arid regions where soil moisture can severely limit vegetation development [10]. Air temperature controls vegetation photosynthesis, and higher temperatures can affect vegetation phenology, extend the growing season, and significantly impact vegetation growth [11]. A study of NDVI changes in Maowusu land sands in China found that temperature and Pre could better explain vegetation dynamics and that the dominant factors varied on different time scales [12]. Qi et al. found that vegetation changes in China's Silk Road Economic Belt were primarily influenced by human activity on 3- and 6-year time scales [13], however, the long-term trend of vegetation changes was primarily influenced by climate change. Chu et al. found that NDVI-based vegetation growing season dynamics in the Mur River–Helongjiang River Basin, located in the middle- and high latitude-parts of eastern Eurasia, are primarily regulated by Pre [14]. Traditional methods based on linearity (linear regression and residual trend analysis) have been widely used in previous studies to reveal the relationships between the monotonic trend of vegetation change and its driving forces. However, the coupled relationship between natural and anthropogenic factors and vegetation change is not linear because of the complex responses of vegetation growth to the driving variables [15,16]. Therefore, rigid linear models cannot accurately describe intrinsic relationship [16]. Moreover, these studies have typically focused on the unilateral effects of natural or anthropogenic factors by identifying correlations between vegetation change and influencing factors. However, the relative importance of these factors in vegetation dynamics has rarely been quantified. In addition, they did not consider the potential interactive effects between the factors affecting vegetation change; however, these methods have limited capabilities. Given that nonlinear effects and interactions make vegetation dynamics relatively complex [17], quantifying the contributions of these underlying factors to vegetation changes remains challenging. In recent years, new models and analysis methods have been developed, including least-squares cross-wavelet analysis [18], support vector machines [19], GeoDetector [20]. GeoDetector is a type of model used to detect spatial dissimilarity without having to follow the linear assumptions of traditional statistical methods. It reveals the mechanism of the independent variable's influence on the dependent variable and has been widely used in the fields of land use [21,22], soil and vegetation ecology [23–28].

The northern foothills of the Yinshan Mountains region are a link between east-central China and the west, and an important ecotonal barrier between the monsoon climate zone in the east and the arid zone in the northwest. With the gradual advancement and expansion of the agricultural zone in the southeast to the pastoral zone in the northwest throughout history, agriculture and livestock production have largely disrupted the natural ecological balance, seriously affecting the income of farmers and herders as well as the development of the local economy. In addition, the harsh natural environment and long-term overcultivation and overgrazing have severely affected biodiversity and ecosystem functions in the agricultural and pastoral areas in the northern foothills of the Yinshan Mountains, causing serious environmental problems such as desertification and farmland degradation [29]. To effectively mitigate these environmental problems, and in response to the Chinese government's project of returning farmland to forest, a series of ecological restoration and management policies and measures, such as ecological fallow and restoration of degraded grasslands, have been implemented in the region, and the ecological and environmental conditions have gradually improved [30]. However, few studies have investigated the vegetation dynamics in the northern foothills of the Yinshan Mountains. In addition, little is known about the potential impact of human activity and other environmental factors on vegetation growth in this region. As a powerful tool for driving force and factor analyses, GeoDetector can quantify driving force and influence of its interaction in a robust and direct manner [31]. Thus, this approach has been successfully used to quantify the impact of driving factors on vegetation change and may be an effective tool for uncovering the causes of vegetation change in terrestrial ecosystems. Using this model, the spatial differentiation of vegetation, the influence of various natural and human factors on the spatial distribution of vegetation, and the types and ranges suitable for vegetation growth were investigated. This study provides a scientific basis for promoting soil and water conservation, vegetation, and ecological restoration in the northern foothills of the Yinshan Mountains.

Based on the above, this study used trend and stability analysis, and GeoDetector methods based on GIMMS NDVI data from 1982 to 2022 to achieve three objectives: (1) to reveal the spatial and temporal characteristics and patterns of NDVI-based vegetation dynamics in the northern foothills of the Yinshan Mountains; (2) to quantify the driving forces for the spatial differentiation of vegetation due to natural factors and human activity; and (3) to determine the appropriate types or ranges of major influencing factors that can contribute to the growth of vegetation in the region. These findings are helpful for a better understanding of the complex mechanisms of vegetation change and for providing scientific suggestions for the prevention of vegetation degradation.

2. Materials and methods

2.1. Study area

The northern foothills of the Yinshan Mountains are located in the northern part of Inner Mongolia, bordering Mongolia, and belong to the transitional zone between the Yinshan Mountains and the Mongolian Plateau, which is a typical agro-pastoral ecotone. The geographic location of the study area is 105.20°E–116.91°E, 40.55°N–45.44°N, and covers an area of approximately 217,637 km^2 (Fig. 1). Most of the area has an arid and semi-arid climate, with average Pre between 100 and 400 mm annually, average annual Win of 2–6 m/s, and the number of days with gale force winds of level 8 or above is 20–80 d annually [32]. The primary vegetation types and their area percentages in the study area are desert (22.02 %), grassland (64.34 %), meadow (7.44 %), scrub (4.56 %), and woodland (1.64 %) [33]. The soil distribution in the study area displays obvious zonational and belongs to the transitional soil type from typical grassland to desert grassland. The northern and northwestern regions of the study area have brown calcareous soil, the southern region has chestnut calcareous soil, and the central region has light chestnut calcareous soil. Soil thickness and fertility decrease from south to north. Most grasslands in the area are severely degraded with a simple ecosystem structure, weak self-regulation and recovery ability, extreme vulnerability to human interference and natural disasters, poor water resources, an extremely fragile ecological environment, a high proportion of wind-eroded and sandy land, and a major source of sandstorms that pose a threat to the ecological security of Northern China.

2.2. Data sources and processing

2.2.1. NDVI data

NDVI data have a linear or almost linear relationship with green leaf density, photosynthetically active radiation, vegetation productivity, and plant biomass and are recognized as effective indicators of vegetation growth state and coverage [34]. NASA's Global Monitoring and Modeling Research Group has recently released the third generation of its Global Vegetation Index product, GIMMS NDVI3g v1.2 (GIMMS-3G+), for 1982–2022, with a temporal resolution of a half month and a spatial resolution of 0.0833° [35]. To ensure data quality, the GIMMS NDVI dataset underwent rigorous radiometric calibration, geometric, solar zenith angle and atmospheric correction, cloud screening, and correction of the most frequently dropped scan lines to ensure data quality [36,37]. Compared to other NDVI datasets (SPOT VGT and MODIS NDVI), this dataset has the advantages of long time series, high precision, and little error (RMSE ±0.005 NDVI units), and has good applicability in global and regional vegetation phenology studies [38,39]. The dataset used in this study was China's 8-km resolution monthly NDVI dataset (1982–2022), which was primarily obtained from the National Earth System Science Data Center (http://www.geodata.cn). ArcGIS 10.7 software was used to transform the monthly dataset into the annual NDVI dataset required for this study area using maximum synthesis, transprojection, and cropping.

2.2.2. Influencing factor data

We categorized the 26 variables affecting vegetation dynamics into five groups: climate, human activity, topography, soil and vegetation type. The climate data were primarily based on the daily observation data of meteorological elements from more than 2400 stations across the country, which were interpolated using the smooth spline function of the ANUSPLIN meteorological interpolation software. Eight major meteorological elements were included as their annual averages: Pre, evaporation, relative humidity (Rhu), air temperature, soil temperature, sunshine hours, Win and air pressure. Human activity include China's gross domestic product (GDP)

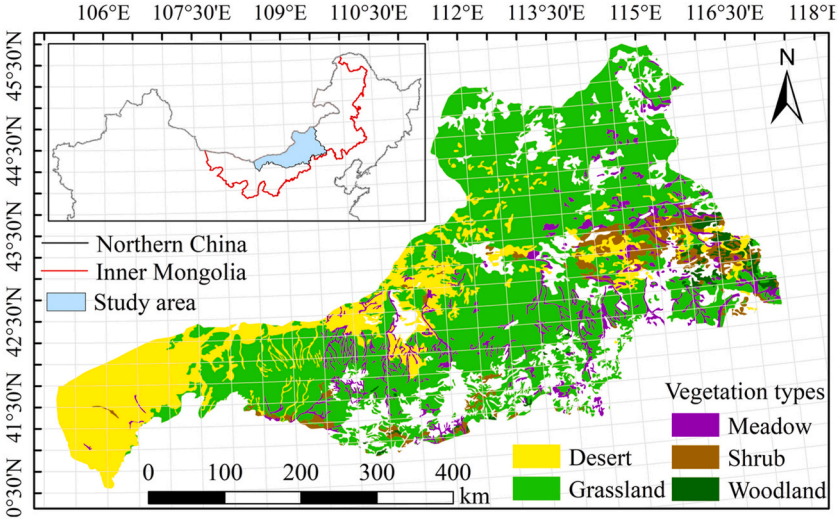

Fig. 1. Vegetation types and location of the northern foothills of the Yinshan Mountains, Inner Mongolia.

and population kilometer-gridded spatial distribution datasets. Topographic factors, including elevation, aspect and slope, were extracted from a digital elevation model (DEM) with 90 m resolution provided by the Geospatial Data Cloud (http://www.gscloud.cn/). The soil data included type, texture, and erosion conditions. Soil type data were obtained from the 1:1,000,000 Soil Map of the People's Republic of China, compiled and published by the National Soil Census Office in 1995. Soil texture data were obtained from the 1:1,000,000 Soil Type Map, and soil profile data on sandy, powdery, and sticky grain content were obtained from the Second Soil Census. Soil erosion data were obtained from "Spatial Distribution Data of Soil Erosion in China", which was compiled in accordance with the general requirements of the Industry Standard SL190-96 of the People's Republic of China, "Classification and Grading Standards for Soil Erosion". The spatial distribution of vegetation types was obtained from a Vegetation Map of the People's Republic of China (1:1,000,000) [40]. All the above data were obtained from the Resource and Environment Science Data Center of the Chinese Academy of Sciences (http://www.resde.cn/). In addition, annual records of the global Human Footprint from 2000 to 2018 are freely available in the figshare repository (https://doi.org/10.6084/m9.figshare.16571064) [41]. Remote-sensing data for nighttime lights were primarily derived from the China Long Time Series Artificial Nighttime Lights Dataset (1984–2020) of the National Tibetan Plateau Science Data Center (http://data.tpdc.ac.cn/) [33]. We obtained raster maps of soil organic matter, soil total nitrogen (STN), soil total phosphorus, and soil total potassium (STK) contents in China at a spatial resolution of 1 km from the National Earth System Science Data Center (http://soil.geodata.cn/).

We ensure consistency in spatiotemporal resolution by averaging the NDVI and 26 variables over 1982–2022. This method has been widely applied to analyze vegetation dynamics in several regions, including the Chengdu–Chongqing region [42] and the China–Myanmar Economic Corridor in China [43]. In order to meet the input requirements of the Geo-Detector, we divided the vegetation type data into five categories, defined as desert, forest, scrub, grassland, and meadow; the slope type data were divided into nine categories, defined as flatland, north, northeast, east, southeast, south, southwest, west, and northwest divisions; soil type data were divided into nine categories, defined as semi-glacial, calcareous, arid, desert, primordial, semi-hydromorphic, hydromorphic, saline, and non-soil types; and soil erosion data were divided into six categories, defined as mild and intense hydraulic, mild wind, moderate wind, intense wind, and freeze–thaw erosion. The remaining factors influencing NDVI were uniformly classified into six categories using the natural discontinuity method. We created an 8 km fishing net in ArcGIS 10.7 software, then extracted the NDVI to the points, removed outliers to create a suitable attribute table for geoprobes, and calculated it using the geoprobe model.

2.3. Research methods

2.3.1. Trend analysis

In this study, Theil–Sen median method and M − K methods were used for trend analysis and significance tests of the NDVI changes, respectively. Theil–Sen median trend analysis is a non-parametric statistical method that has the advantage of not requiring samples to follow a specific distribution, is computationally efficient and insensitive to outliers without compromising its accuracy and has a strong ability to avoid measurement errors or anomalies [44]. A comparison of different linear regression models has shown that this method has significant advantages in the case of small sample sizes [5]. This is calculated as follows:

$$Slope_{NDVI} = Median\left(\frac{NDVI_j - NDVI_i}{j - i}\right)$$

In the formula, $Slope_{NDVI}$ represents the trend of NDVI, $NDVI_j$ and $NDVI_i$ are the NDVI values in the jth and ith years of the image element, respectively, when $Slope_{NDVI} > 0$, it indicates that the NDVI shows an increasing trend, and vice versa shows a decreasing trend. If $Slope_{NDVI} = 0$, NDVI remains stable.

The M − K test is a non-parametric test, which means that no prior assumptions regarding the statistical distribution of data are required [45,46]. The normalized statistic Z was primarily used to test the trends and significance of the time series. It is generally accepted that $|Z| \geq 1.96$, which indicates that the significance test is passed. For the specific methodology of the M − K test [47].

2.3.2. Spatial stability analysis

In this study, the coefficient of variation (CV) was used to reflect the degree of variation in NDVI, and the calculation was performed as follows:

$$CV = \frac{\sqrt{\sum_{i=1}^{n}(NDVI_i - \overline{NDVI})^2/(n-1)}}{\overline{NDVI}}$$

Where $\overline{NDVI}$ is the average value of *NDVI* over the period 1982–2022.

2.3.3. Hurst exponent and R/S analysis

The R/S analysis is used to estimate the Hurst exponent [48], which is used to predict the future evolutionary trend of NDVI in this study, the main calculation procedures were as follows [49]. The time series (of returns) of length L must be divided into d sub series ($Z_{i,m}$) of length n, and for each sub series $m = 1, \ldots, d$. Then.

1. It is necessary to determine the mean (E_m) and standard deviation (S_m) of the sub series ($Z_{i,m}$).
2. The data of the sub series ($Z_{i,m}$) has to be normalized by subtracting the sample mean $X_{i,m} = Z_{i,m} - E_m$ for $i = 1, \ldots, n$.

3. Create a cumulative time series $Y_{i,m} = \sum_{i=1}^{i} X_{j,m}$ for $i = 1, \ldots, n$.
4. Find the range $R_m = \max\{Y_{1,m}, \ldots, Y_{n,m}\} - \min\{Y_{1,m}, \ldots, Y_{n,m}\}$.
5. Rescale the range (R_m/S_m).
6. Calculate the mean value $(R/S)_n$ of the rescaled range for all sub series of length n.

Considering that the R/S statistic asymptotically follows the relation $(R/S)_n \approx cn^H$, the value of H can be obtained by running a simple linear regression over a sample increasing time horizons.

$$\log (R/S)_n = \log c + H \log n$$

The Hurst exponent ranges from 0 to 1; when $0<H < 0.5$, the time series has a long-term correlation, but the general trend in the future is opposite to the past, that is, antipersistence. If a time series moves upward in the first period, it is likely to move downward in the next period, and vice versa. The strength of this antipersistence behavior depends on how close H is to zero; the closer it is to zero, the more negatively correlated it is. When $H = 0.5$, the time series is random and uncorrelated, and the present does not affect the future. If $H > 0.5$, the time series is characterized by long-term correlation, that is, the process is persistent. The closer H is to 1, the stronger the correlation. If a series moves up in the previous period, it continues to move up in the next period. When $H = 1$, the future is perfectly predictable with respect to the present [48,50].

2.3.4. GeoDetector model

GeoDetector is an open-source statistical model for spatial data analysis (http://www.GeoDetector.cn/) that is used to determine the similarity of the spatial distribution of two variables by considering spatially stratified heterogeneity. GeoDetector consists of factor, interaction, risk, and ecological detectors.

2.3.4.1. Factor detector. Factor detection was used to determine the extent to which each factor explaind the spatial variability of NDVI(Y) and is calculated using the following formula:

$$q = 1 - \frac{1}{N\sigma^2} \sum_{h=1}^{L} N_h {\sigma_h}^2$$

where $h = 1, 2, \ldots,$ p. L is the stratification of the variable (Y) or factor (X); N_h and N are the number of cells in stratum h and in the entire region, respectively; σ_h^2 and σ^2 are the variances of the values of (Y) in stratum h and in the whole region, respectively. q takes values in the range [0, 1]. q has a greater explanatory power for factor (X) over variable (Y) the greater the value of q. $q = 0$ means that the two are not related.

2.3.4.2. Interaction detector. Factor interaction detector was used to determine whether two factors interact on the dependent variable Y, i.e., whether the two factors together increase or decrease the explanatory power of NDVI, and the types of interactions are shown in Table 1.

2.3.4.3. Risk detector. The t-statistic test is used to determine the type or appropriate range of influence of each factor on the vegetation cover. The specific formula is as follows:

$$t_{\bar{y}_{h=1} - \bar{y}_{h=2}} = \frac{\overline{Y}_{h=1} - \overline{Y}_{h=2}}{\left[\frac{Var(\overline{Y}_{h=1})}{n_{h=1}} + \frac{Var(\overline{Y}_{h=2})}{n_{h=2}}\right]^{1/2}}$$

Where $\bar{Y}_h$ is the mean of the attribute in subregion h, n_h is the number of samples in subregion h, and Var is the variance. Statistic t approximately follows the Student's t distribution, where the degrees of freedom are calculated as:

$$df = \frac{\frac{Var(\overline{Y}_{h=1})}{n_{h=1}} + \frac{Var(\overline{Y}_{h=2})}{n_{z=2}}}{\frac{1}{n_{h=1}-1}\left[\frac{Var(\overline{Y}_{h=1})}{n_{h=1}}\right]^2 + \frac{1}{n_{h=2}-1}\left[\frac{Var(\overline{Y}_{h=2})}{n_{h=2}}\right]^2}$$

Table 1
Types of GeoDetector factor interactions.

Types of interaction	Descriptions
Non-linear reduction	q(X1∩X2) < Min(q(X1), q(X2))
Single-factor non-linear reduction	Min(q(X1), q(X2)) < q(X1∩X2) < Max(q(X1), q(X2))
Two-factor enhancement	q(X1∩X2) > Max(q(X1), q(X2))
Independent	q(X1∩X2) = q(X1) + q(X2)
Non-linear enhancement	q(X1∩X2) > q(X1) + q(X2)

The null hypothesis H_0: $\bar{Y}_{h=1} = \bar{Y}_{h=2}$, if H_0 is rejected at the confidence level α, then the means of the attributes between the two subregions are significantly different.

2.3.4.4. Ecological detector. An ecological detector was used to compare whether the effects of factors $X1$ and $X2$ on the spatial distribution of attribute Y were significantly different, as measured by the F-statistic:

$$F = \frac{N_{X1}(N_{X2}-1)SSW_{X1}}{N_{X2}(N_{X1}-1)SSW_{X2}}$$

$$SSW_{X1} = \sum_{h=1}^{L_1} N_h {\sigma_h}^2$$

$$SSW_{X2} = \sum_{h=1}^{L_2} N_h {\sigma_h}^2$$

Where N_{X1} and N_{X2} denote the sample sizes of the two factors $X1$ and $X2$, respectively, SSW_{X1} and SSW_{X2} denote the sum of the within-stratum variances of the strata formed by $X1$ and $X2$, respectively, and $L1$ and $L2$ denote the number of strata of variables $X1$ and $X2$, respectively. The null hypothesis was H_0: $SSW_{X1} = SSW_{X2}$. If H_0 is rejected at a significance level of α, this indicates that there is a significant difference between the effects of the two factors $X1$ and $X2$ on the spatial distribution of attribute Y.

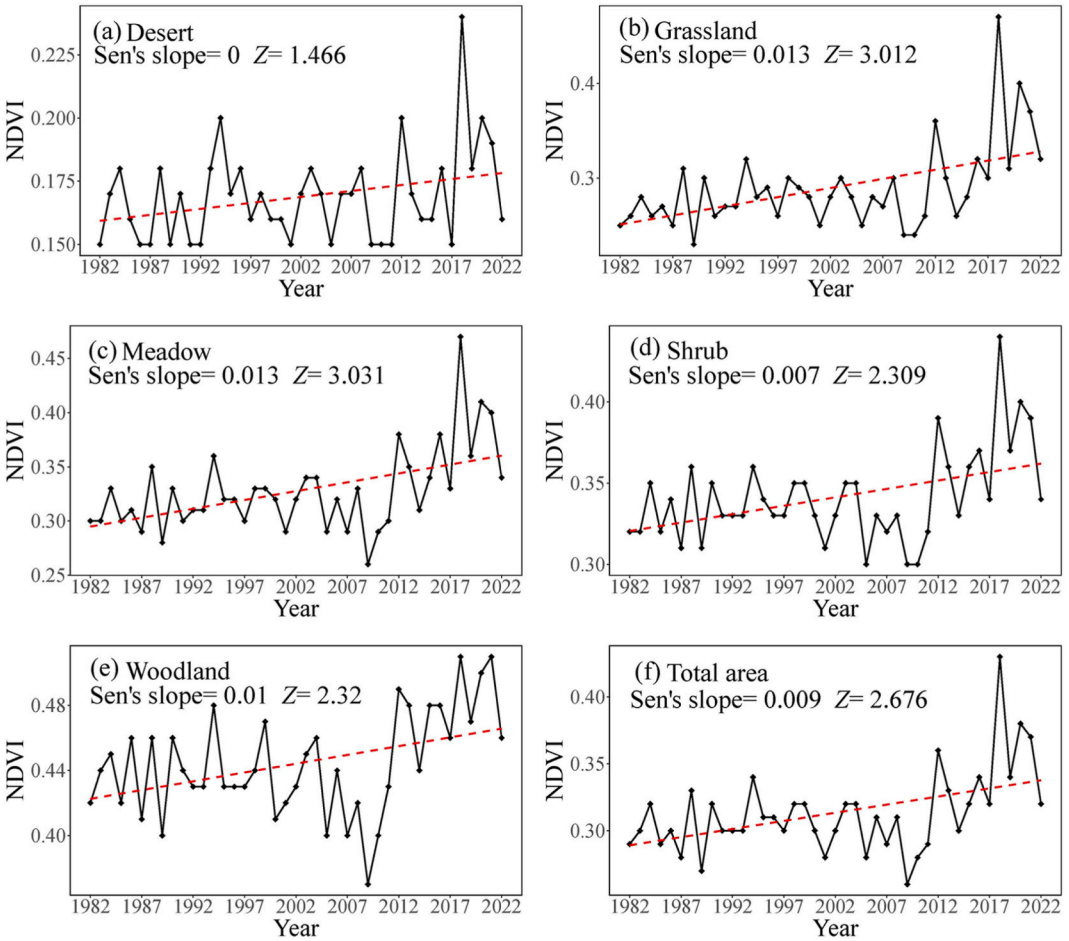

Fig. 2. Interannual variation of NDVI in the northern foothills of the Yinshan Mountains from 1982 to 2022.

3. Results

3.1. Vegetation dynamic trend during 1982–2022

Changes in the mean NDVI values in the northern foothills of the Yinshan Mountains were analyzed on an annual time scale. As shown in Fig. 2, the NDVI in the study area showed a significant increasing trend during the period of 1982–2022, with a growth rate of 0.0091/decade. Except for the desert NDVI, which showed no significant change, all other vegetation types showed a significant increasing trend. The growth rate of the NDVI was in the following order: grassland (0.0135/decade) > meadow (0.0133/decade) > woodland (0.01/decade) > scrubland (0.0069/decade). Hence, there has been a general trend of improvement in the vegetation cover in the northern foothills of the Yinshan Mountains over the past 40 years.

3.2. Spatial distribution pattern of NDVI

Based on the 1982–2022 NDVI time series data, 41-year averages were calculated pixel-by-pixel to obtain the mean NDVI values for each image (Fig. 3a). In this study, the vegetation condition of the study area was classified into five types using the natural discontinuity classification (Jenks): very low vegetation cover (0.08–0.17), low vegetation cover (0.18–0.25), medium vegetation cover (0.26–0.34), high vegetation cover (0.35–0.44), and very high vegetation cover (0.45–0.71) (Fig. 3b). The spatial distribution of NDVI in the grassland area of the northern foothills of the Yinshan Mountains was generally high in the east and low in the west. The very low vegetation cover area accounted for 13.23 % of the total study area and was primarily located in the westernmost part of the

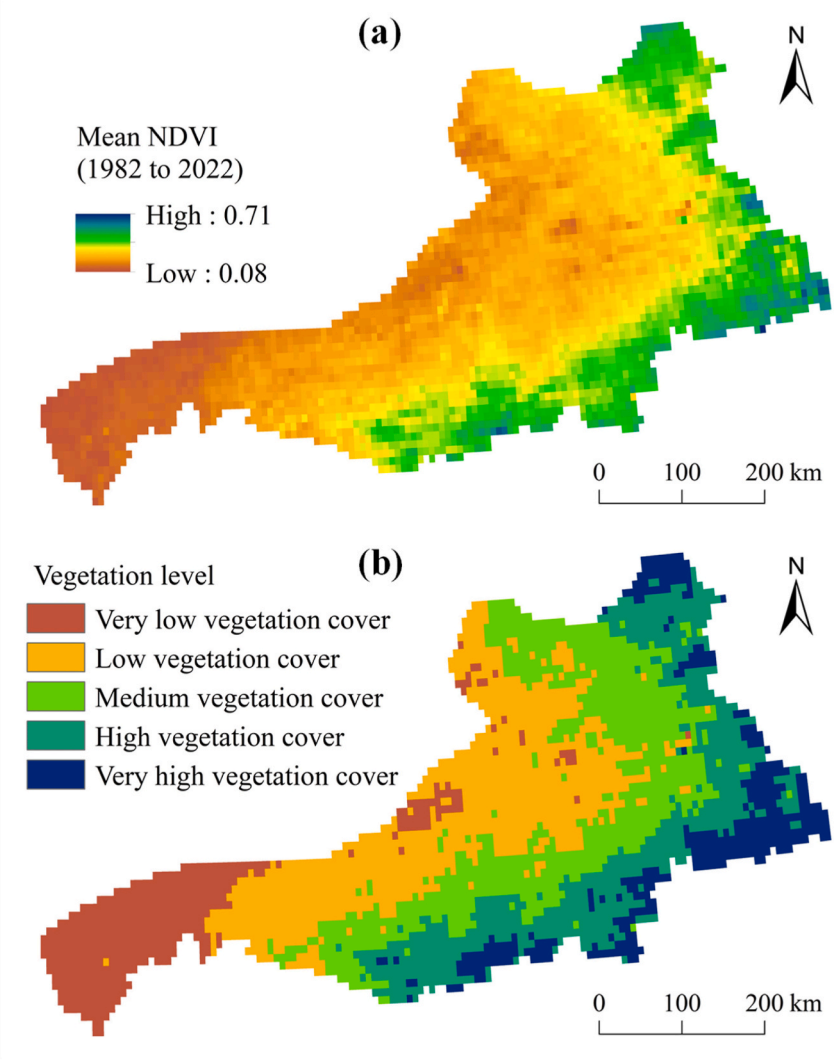

Fig. 3. Multi-year vegetation NDVI values and spatial distribution of vegetation in the northern foothills of the Yinshan Mountains.

study area, where the dominant vegetation type was desert landscape. The vegetation condition was primarily dominated by low and medium vegetation cover, which accounted for 30.29 % and 25.72 % of the total study area, respectively, and were primarily distributed in the central part of the study area. High and very high vegetation cover accounted for 20.16 % and 10.60 % of the total study area, respectively, and were primarily distributed in the eastern and southern edges of the study area, respectively.

3.3. NDVI spatial stability analysis

The CV of the NDVI in the study area was calculated pixel-by-pixel for 1982–2022 and divided by the natural discontinuity classification (Jenks) (Fig. 4). Very low- and low-volatility vegetation accounted for 19.32 and 30.78 % of the total study area, respectively. Medium-volatility vegetation accounted for 26.88 % of the total study area. High-volatility and extremely high-volatility vegetation accounted for 17.87 and 5.15 % of the total study area, respectively, and the overall NDVI changes showed a trend of low and medium volatility, with great variability across the study area.

3.4. Spatial pattern of vegetation dynamic trend

Based on the results of the Theil–Sen median trend analysis, changes in the NDVI of the study area were categorized as improved, stabilized, and degraded according to slope >0, slope $= 0$, and slope <0, respectively. The results of the M − K test at 0.05 confidence level were categorized into significant and non-significant changes according to $|Z|>1.96$ and $|Z|<1.96$. The Theil–Sen median trend and M − K test classification results spatially overlapped, and the NDVI changes were finally classified into five categories: significant and slight improvement, stability, slight and significant degradation according to the coupling results (Fig. 5), and statistics on the proportion of area of each type of change trend according to different vegetation types (Table 2).

Fig. 5 and Table 2 show that the trend of vegetation change in the northern foothills of the Yinshan Mountains from 1982 to 2022 was dominated by improvement. The improved area accounted for 83.87 % of the total study area, of which the significantly improved area accounted for 43.90 % of the total area, and it was primarily distributed in the eastern and southern region of the study area. The degraded area accounted for 15.21 % of the total study area, with slight degradation accounting for 11.82 % of the total area. The degraded areas were primarily distributed in the western and central region of the study area.

3.5. Trends in future vegetation dynamics

After R/S analysis, the Hurst index mean value was 0.60 (>0.50) in the entire study area, indicating that the vegetation in the northern foothills of the Yinshan Mountain has long-term memory in time series (sustainability). The classification results showed that the area with $0.5 < H < 1$ accounted for 89.26 % of the total study area, and the NDVI in this area was characterized by isotropic sustainability, that is, the future changes in NDVI could continue the 1982–2022 trend. The area with $0 < H < 0.5$ accounted for 10.74 % of the total area, and the vegetation NDVI in this area was characterized by reverse persistence, that is, the future changes in vegetation cover may be contrary to the 1982–2022 trend. Furthermore, the NDVI spatial trends and sustainability spatial patterns were overlaid to create a map of the projected future NDVI trends (Fig. 6). Based on the analysis results, the future developmental trend of vegetation cover in the northern foothills of the Yinshan Mountains was categorized into four directions: worsening, positive, uncertain, and stable (Table 3). Areas with significant improvement in vegetation sustainability were the largest, accounting for 43.79 % of the total area, followed by areas with slight improvement in sustainability, accounting for approximately 33.62 % of the total

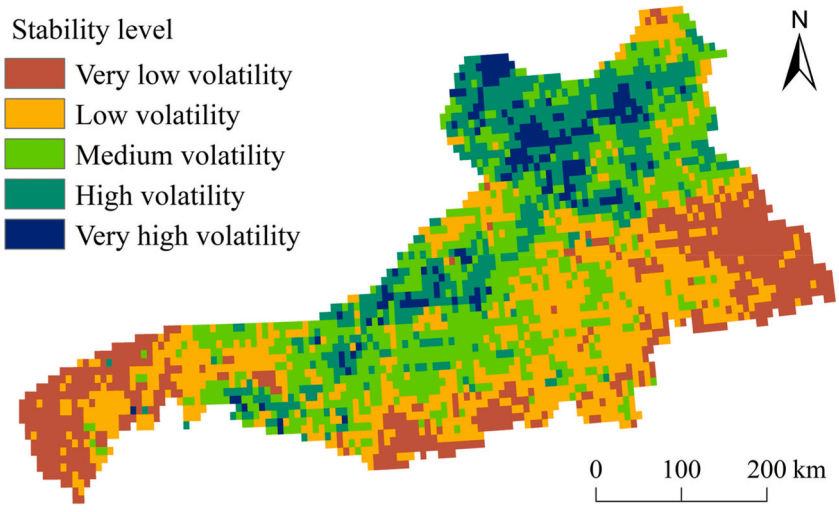

Fig. 4. Spatial fluctuation of NDVI in the northern foothills of the Yinshan Mountains.

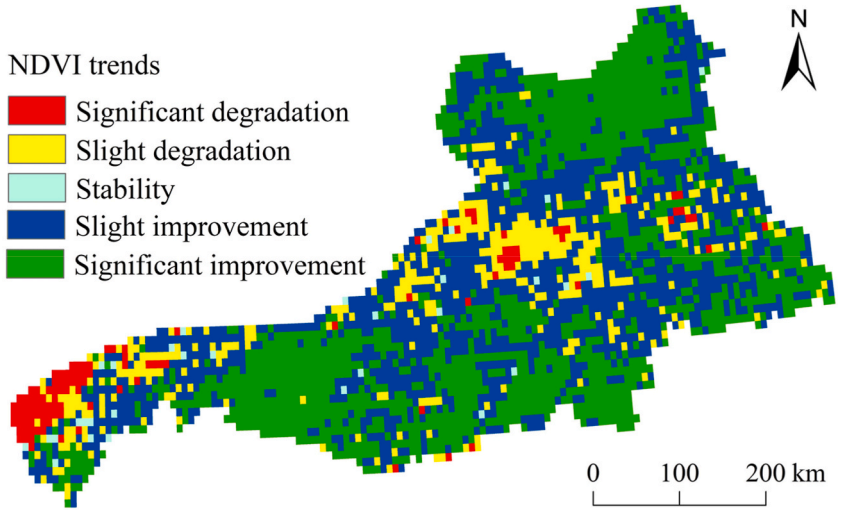

Fig. 5. Trends in NDVI in the northern foothills of the Yinshan Mountains from 1982 to 2022.

Table 2
Area proportion of vegetation change trend in the northern foothills of the Yinshan Mountains during 1982–2022.

Slope	Z	Trends	Desert	Grassland	Meadow	Scrub	Woodland	Total area
<0	>1.96	Significant degradation	13.17 %	1.03 %	0.48 %	3.91 %	2.33 %	3.39 %
<0	−1.96 to 1.96	Slight degradation	19.67 %	10.55 %	8.10 %	14.84 %	16.28 %	11.82 %
0	−1.96 to 1.96	Stability	2.28 %	0.81 %	0.00 %	0.00 %	0.00 %	0.93 %
>0	−1.96 to 1.96	Slight improvement	44.39 %	38.07 %	44.29 %	44.53 %	37.21 %	39.97 %
>0	< −1.96	Significant improvement	20.49 %	49.54 %	47.14 %	36.72 %	44.19 %	43.90 %

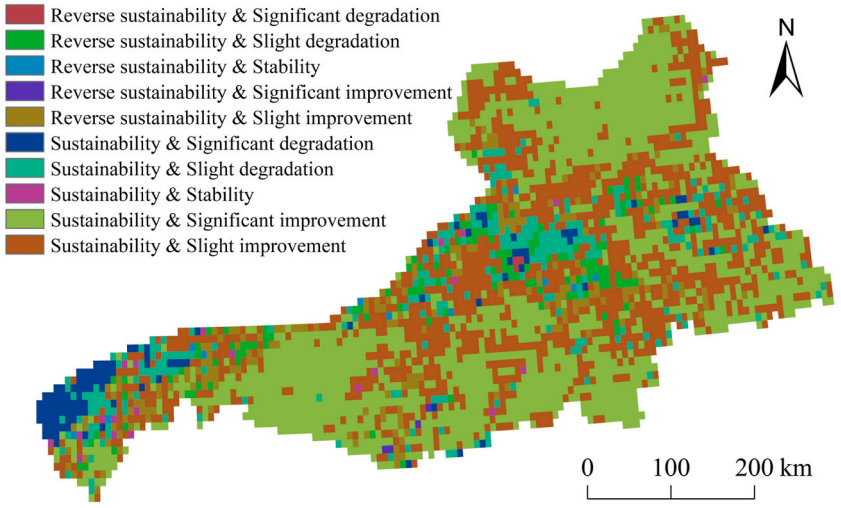

Fig. 6. Future vegetation trends in the northern foothills of the Yinshan Mountains.

area. Areas of slight degradation in vegetation sustainability accounted for 7.94 % of the total area, areas of slight improvement in reverse sustainability accounted for 6.34 % of the total area, and other future development trends accounted for a smaller percentage of the area <5 %.

3.6. Factors influencing the spatial distribution of NDVI

3.6.1. Factor detector analysis

The factor detector results for the GeoDetector used in this study are listed in Table 4. The ability of each factor to explain the spatial

Table 3
Area proportion of the NDVI direction of vegetation in the northern foothills of the Yinshan Mountains.

Future directions	Future trends	Area proportions
Worsening direction	Sustainability and significant degradation	3.30 %
	Sustainability and slight degradation	7.94 %
	Reverse sustainability and significant improvement	0.12 %
	Reverse sustainability and slight improvement	6.34 %
Positive direction	Sustainability and significant improvement	43.79 %
	Sustainability and slight improvement	33.62 %
	Reverse sustainability and significant degradation	0.09 %
	Reverse sustainability and slight degradation	3.88 %
Uncertain	Reverse sustainability and stability	0.32 %
Stable	Sustainability and stability	0.61 %

Table 4
Results of factor detector.

Factors	Vegtype	Pre	Evp	Rhu	Tem	Ssd	Win	Prs	Panda	Hfp	Pop	GDP
q statistic	0.30	0.73	0.80	0.79	0.58	0.75	0.39	0.15	0.01	0.26	0.02	0.01
p value	0.000	0.000	0.000	0.000	0.000	0.000	0.000	0.000	0.94	0.000	0.02	0.01
Factors	Dem	Aspect	Slope	Soiltype	STP	STN	STK	SOC	Silt	Sand	Clay	Erosion
q statistic	0.16	0.02	0.06	0.48	0.11	0.50	0.35	0.45	0.34	0.32	0.30	0.13
p value	0.000	0.000	0.000	0.000	0.000	0.000	0.000	0.000	0.000	0.000	0.000	0.000

distribution of NDVI in the northern foothills of the Yinshan Mountains differed. Among them, annual Pre, evapotranspiration (Evp), Rhu, and sunshine hours (Ssd) all had >70 % explanatory power, with 73.5, 79.9, 79.0, and 74.9 %, respectively. Therefore, meteorological elements were the primary influences on the spatial differentiation of NDVI in the study area. In addition, the explanatory powers of the annual mean temperature (Tem) and STN content were 58.2 and 50.4 %, respectively. The explanatory power of soil

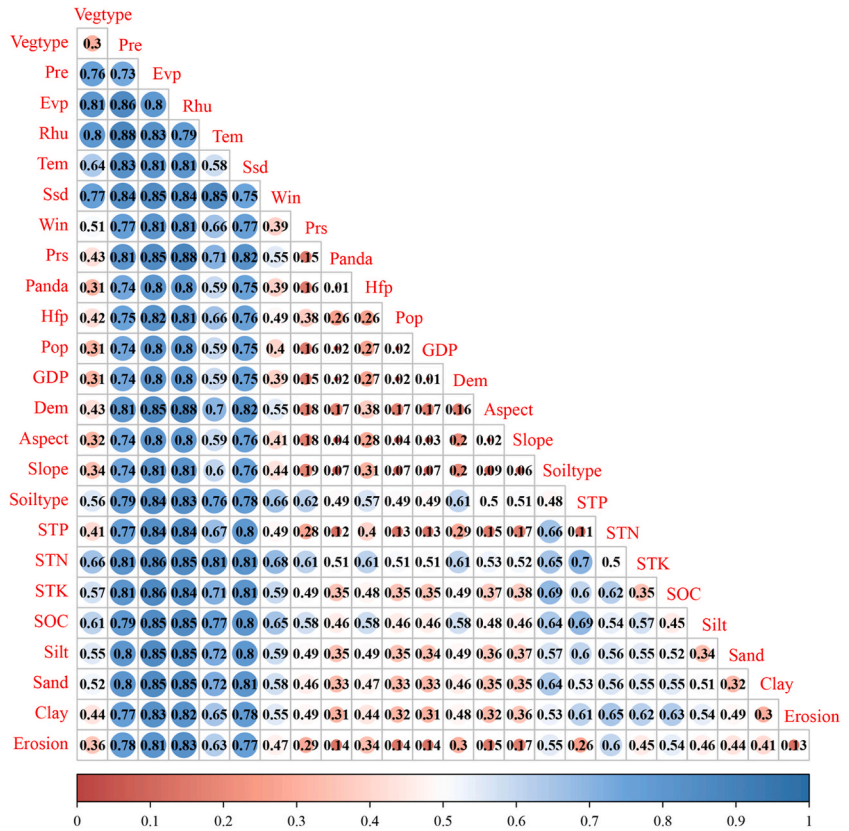

Fig. 7. Influence matrix diagram based on interaction detector analysis.

type, soil organic carbon (SOC) content, STK content, soil silt fraction, sand fraction and Win were all >30 %; therefore, influence of soil elements on the spatial distribution of NDVI could not be ignored. Anthropogenic factors, including terrestrial human footprints (Hfp), nighttime brightness (Panda), population density (Pop), and GDP density, had little influence on the spatial differentiation of the NDVI, indicating that anthropogenic activity was not a dominant factor in vegetation growth in the northern foothills of the Yinshan Mountains.

3.6.2. Interaction detector analysis

The results of the interaction detector analysis showed nonlinear strengthening for any two factors; that is, it was manifested as the sum of the q-values of the two factors being greater than the q-value of the single factor (Fig. 7). The top 10 interactive effects were: Rhu∩Prs (0.8785) > Rhu∩Dem (0.8779) > Pre∩Rhu (0.8759) > Evp∩STN (0.8637) > Evp∩STK (0.8619) > Pre∩Evp (0.8614) > Rhu∩STN (0.8544) > Evp∩Sand (0.8537) > Evp∩Dem (0.8530) > Evp∩Prs (0.8526). Although the independent explanatory power of barometric pressure was low (q = 0.15), the interaction explanatory power of Rhu and barometric pressure was the highest. In addition, the individual explanatory power of elevation was q = 0.16, whereas the independent explanatory powers of Rhu and elevation were 0.8779.Tn addition, STN, STK, and sand fractions had low independent explanatory power, but showed strong explanatory power after interacting with climatic factors. This also confirmed that climatic factors dominated in the spatial variability of the NDVI, whereas elevation and soil factors were important indirect factors influencing the spatial differentiation pattern of the NDVI.

3.6.3. Ecological detection analysis

Ecological tests indicated a significant difference between the effect of the interaction between two factors on vegetation NDVI and the effect of a single factor. The results of this study showed no significant difference in the explanatory power of most combinations of climatic factors on NDVI changes (Fig. 8), which was because climatic factors, as dominant vegetation NDVI factors in the study area, already had high explanatory power individually, making it difficult for climatic factors to combine with each other to produce significant differences.In contrast, the anthropogenic (Panda, Pop, GDP) and topographic factors (Dem, Aspect, Slope), which had very low explanatory power individually, produced significant differences when combined with other factors.

3.6.4. Risk detection analysis

Risk detection analyses evaluated which type or range of influencing factors were more appropriate for vegetation growth as vegetation NDVI changes in response to different factors. The indicate that woodland had the best vegetation cover (Table 5).

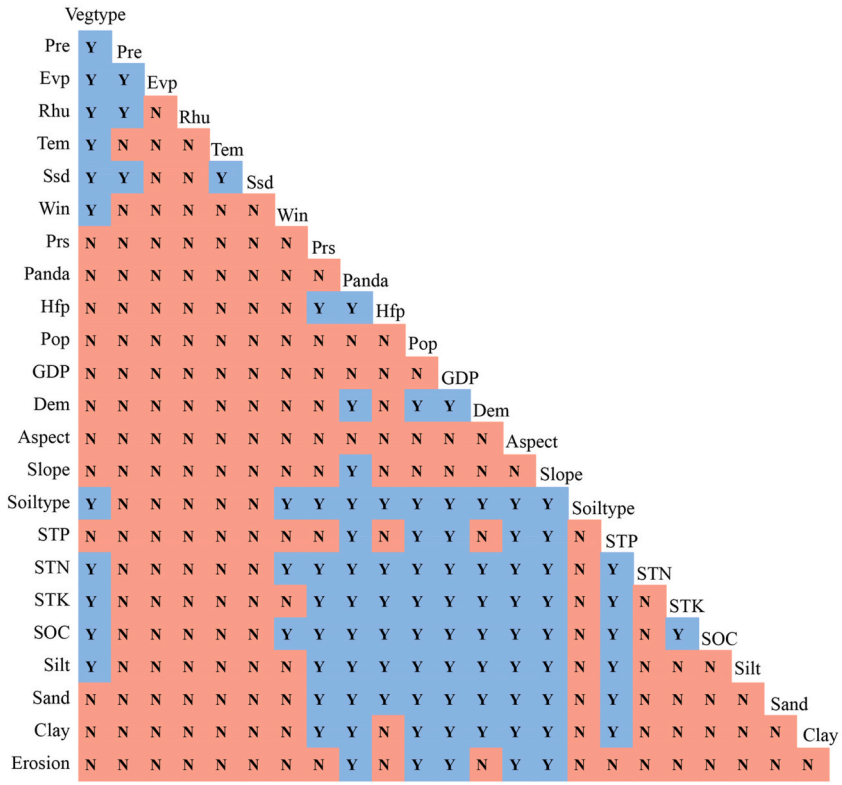

Fig. 8. Ecological detection results.

Table 5
Suitable ranges or types of influencing factors based on risk detection analysis.

Categories	Abbreviations	Unit	Suitable range or type	Average NDVI
Vegetation	VET	–	Woodland	0.443
Climate	Pre	mm	355.61 to 517.28	0.477
	Evp	mm	1538.41 to 1895.69	0.437
	Rhu	%	55.60 to 59.91	0.433
	Tem	°C	−1.76 to 1.00	0.430
	Ssd	hour	2876.50 to 2986.58	0.467
	Win	m/s	3.39 to 3.68	0.376
	Prs	hPa	774.59 to 831.71	0.339
Human activity	Panda	DN	1.20 to 5.31	0.352
	Hfp	–	17.89 to 27.80	0.373
	Pop	person/km^2	1023 to 4014	0.388
	GDP	10^4yuan/km^2	744.54 to 4982.69	0.333
Topography	Dem	m	1686 to 2331	0.352
	Aspect	–	Southwest	0.283
	Slope	°	8.83 to 26.79	0.412
Soil	Soiltype	–	Semi-Luvisols	0.453
	STP	g/kg	1.08 to 1.50	0.420
	STN	g/kg	1.47 to 3.42	0.459
	STK	g/kg	21.68 to 24.20	0.430
	SOC	g/kg	3.06 to 5.78	0.438
	Silt	%	29 to 36	0.370
	Sand	%	40 to 48	0.371
	Clay	%	24 to 29	0.371
	Erosion	–	Mild hydraulic erosion	0.409

Climatically, vegetation NDVI increased with increasing mean annual Pre and mean annualRhu, with optimum intervals ranging from 355.61 to 517.28 mm and 55.60–59.91 %, respectively. However, vegetation NDVI tended to decrease with increasing mean Evp, mean annual Tem, mean annual Ssd, mean annual Win, and mean annual air pressure, whose optimum intervals were 1538.41 to 1895.69 mm, −1.76 to 1.00 °C, 2876.50 to 2986.58 h, 3.39–3.68 m/s, and 774.59 to 831.7 hPa, respectively. In terms of human activity, NDVI was higher in areas with lower night light intensity, Hfp, Pop, and GDP density, with optimal ranges of 1.20–5.31DN, 17.89 to 27.80, 1023 to 4014 persons/km^2, and 744.54 to 4982.69 10^4yuan/km^2,respectively Topographically, the vegetation NDVI increased with increasing elevation and slope, with optimal ranges of 1686 to 2331 m and 8.83–26.79°, respectively, and the optimal slope orientation was southwest. As for soil factors, the most suitable soil type was Semi-Luvisols, with optimum ranges of 40–48 %, 29–36 % and 24–29 % for sand, silt and clay content, respectively. The optimum ranges ofSOC, STN, STK, and total phosphorus contents were 3.06–5.78 g/kg, 1.47–3.42 g/kg, 1.08–1.50 g/kg, and 21.68–24.20 g/kg, respectively, and the optimum type of soil erosion was mild hydraulic.

4. Discussion

4.1. Spatial and temporal changes in vegetation NDVI

The trend of vegetation NDVI change (2001–2018) across Eurasia on the continental scale was reported to be 2.16×10^{-6} per decade [51]. The Inner Mongolian grassland is located in the eastern Eurasian grassland, which is an important part of the Eurasian continent. Wang et al. found that the vegetation NDVI in Inner Mongolia increased significantly by 0.004/10a from 1982 to 2015 [52]. Gao et al. found that the NDVI growth rate of the Inner Mongolian steppe area from 1982 to 2015 was 0.0054/10a, and the change rates of meadow, typical, and desert steppes were 0.0035/10, 0.0061/10, and 0.0037/10a, respectively [53]. Therefore, the NDVI growth rate in this study (0.0091/10a) (Fig. 2) was higher than that of Eurasian vegetation and various grassland types in Inner Mongolia, primarily because grassland has the highest upward trend among ecosystem types [51], Grassland accounted for 64.34 % of the northern foothills of the Yinshan Mountains, and the NDVI change rate of grassland was 0.0135/10a in this study, resulting in a high change rate of NDVI over the entire study area. The overall increasing trend of the NDVI in the northern foothills of the Yinshan Mountains may be attributed to climate change-induced warming and CO_2 fertilization effects [54], particularly in colder regions [55]. This can be attributed to increased Preand ecological protection in Inner Mongolia [56].

4.2. NDVI spatial pattern drivers

In this study, we analyzed the effects of 26 variables, including climate, human activity, topography, soil, and vegetation, on the spatial pattern of the NDVI in the northern foothills of the Yinshan Mountains. Previous studies have confirmed that climatice factors are crucial for vegetation growth and distribution [57,58]. In this study, the results of the factor detector analysis showed that annual Pre, Evp, Rhu, and Ssd all have an explanation rate of >70 %, and the explanatory power of annual Tem was 58.2 % (Table 3), indicating that climatic factors are the dominant NDVI spatial variability drivers in the study area. This result is consistent with the findings of Tian et al. [59], who reported that vegetation growth in most regions of Inner Mongolia is affected by climate change. In

addition, we found that Pre had a greater influence on NDVI spatial patterns than temperature in the study area, confirming the finding of Gao et al. that vegetation productivity in Inner Mongolian grasslands is more sensitive to changes in water conditions than to changes in temperature [53]. This is primarily because the Inner Mongolia Autonomous Region is sensitive to climate change and has experienced long-term warming and drying trends in recent decades [60]. Many studies have reported an increase in the intensity and frequency of droughts in Inner Mongolia owing to increased Evp caused by high temperatures [61,62]. In arid and semi-arid ecosystems characterized by water scarcity and low soil moisture, scarce Pre can dominate vegetation growth. Pre is the dominant factor affecting vegetation productivity in desert grasslands and grassland steppes [63]. Previous studies have generally confirmed the dominant role of moisture conditions on vegetation, rather than radiation and temperature [64–66]. For example, on the water-scarce Loess Plateau, water effectiveness has the greatest effect on grassland productivity [67]. In contrast, the global-scale correlation between temperature and vegetation productivity is strongest in the northern high latitudes [68], supporting the view that temperature dominates the seasonal dynamics of vegetation growth in cooler regions. For example, the alpine meadows on the Tibetan Plateau, which have long been cold, are highly sensitive to rising temperatures [55,69,70]. Among the different ecosystems, grasslands are the most sensitive to Pre, followed by shrublands and croplands, and forests are the least sensitive to Pre [51]. This is primarily becausegrasslands with shallow root systems are more sensitive to drought. In this study, the grassland area in the northern foothills of the Yinshan Mountains in northern Inner Mongolia was mostly characterized by a warm arid climate with high temperature and drought, and soil moisture was primarily dependent on Pre recharge, making Prethe dominant factor affecting vegetation growth in the region.

In this study, the soil type, SOC content, STK content, soil silt fraction and sand fraction explained >30 % of the NDVI (Table 3), and the influence of soil factors on the spatial distribution of NDVI should not be ignored. This is because in arid and semi-arid regions, soil factors, which are important ecological factors for the spatial distribution and growth of vegetation, have a significant effect on vegetation growth and the efficiency of rainfall reuse [71]. Furthermore, plants absorb water and nutrients from the soil through their root systems for growth and metabolism. Minerals provide the nutrients required by plants, such as nitrogen, phosphorus, and potassium, which are essential for the synthesis of cell tissue, proteins, and other biomolecules. Second, the soil has good water retention and aeration, providing appropriate environmental conditions for plant growth. Soil texture alters the exchange of water and heat between the soil and vegetation, thereby affecting the response of vegetation to the climate. The study area is located in an arid and semi-arid zone, where Pre is scarce and evaporation is intense, and Pre is the most important limiting factor for vegetation growth. Soils with a high clay content in the surface layer contain a higher percentage of water than coarse textured soils [72]. Water located in the surface layer of the soil is subjected to strong evaporative losses, resulting in a relatively unstable water resource in the surface layer [73]. This pattern of water distribution concentrated at the soil surface favors plants with shallow root systems, which are highly sensitive to drought [74]. Soils with high clay content (high porosity) have a high water-holding capacity and low permeability (water and air). In clayey soils, a large percentage of the total pore space is microporous, which does not allow rapid water movement and helps plants withstand prolonged drought.

In terms of topography, the q-values of the effects of elevation, slope, and slope direction on the spatial differentiation of NDVI were 0.16, 0.06, and 0.02, respectively (Table 3), which was because the topography of the study area is relatively flat (Fig. 9), resulting in very little difference in vegetation growth. In terms of human activity, the impact on the vegetation of the Inner Mongolia Plateau was mostly positive, which was largely related to the implementation of a series of local ecological projects in recent years. Since 2003, the government has implemented “No grazing and resting on pasture” and “Grass-animal balance” policies in the region, together with the "Tianjin-Hebei wind and sand source" management project in the region, which has effectively mitigated grassland degradation on the Inner Mongolia Plateau. In this study, we found that anthropogenic factors such as Hfp, Panda, Pop, and GDP density had little influence on the spatial variation of NDVI, which was due to the sparse population in this study area, and it may be related to selected human activity indicators.

4.3. Uncertainties and limitations

The vegetation index is a simple and effective parameter used in remote sensing to characterize vegetation cover on the ground surface, and is widely used in studies on vegetation type, growth, and vegetation cover monitoring, including biomass estimation. NDVI, an important indicator for monitoring changes in ground vegetation, partially removes the effects of radiative changes related to atmospheric conditions such as the sun elevation and satellite observation angles, topography, and cloud shadows [75], and has been widely used in global and regional land cover, vegetation classification and change, primary productivity analysis, and drought monitoring. However, it has some shortcomings that cannot be ignored. For example, NDVI has low sensitivity in areas with high vegetation cover and cannot accurately detect vegetation loss during short-term extreme climatic events [76]. In addition, the NDVI overestimates the vegetation cover at the beginning and end of the growing season. Therefore, future research should comprehensively analyze and evaluate the uncertainty characteristics of multi-source vegetation remote sensing products, such as the consistency evaluation of vegetation dynamic characteristics in this study area using three NDVI datasets, namely GIMMS, MODIS, and SPOT, to reasonably interpret the monitoring results and ensure the accuracy of the vegetation production status assessment.

In this study, we used GeoDetector to analyze the driving factors of the NDVI spatial variability of grassland in the northern foothills of the Yinshan Mountains in Inner Mongolia, which allowed us to quantitatively study the effects of numerical and qualitative data driving factors on the NDVI of grassland in the study area. However, because of the complexity of the impact of human activitiy on the vegetation cover of grasslands, particularly the management mode, structure and density of livestock, and the intensity of grazing, the growth of grassland vegetation will have a certain impact on the growth of grass. The impact of human activity on grassland vegetation cover is very complicated. At the same time, factors that are difficult to quantify, such as grassland fires and rodent and insect disasters, will also affect grassland vegetation cover, and these factors have not been considered in this study. Otherrelevant factors affecting

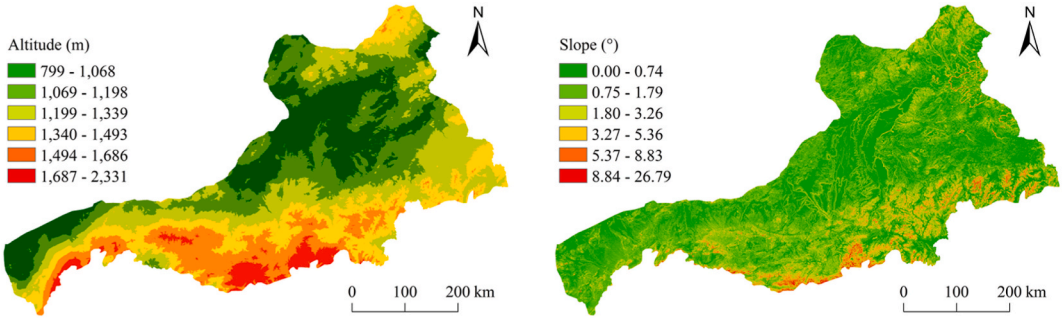

Fig. 9. Spatial distribution of elevation and slope in the study area.

grassland vegetation cover should be selected in future studies to investigate the driving mechanism of vegetation cover changes in depth.

5. Conclusions

In this study, based on 1982–2022 GIMMS NDVI, soil, meteorological and topographic data, we analyzed the spatial and temporal characteristics of vegetation cover and the driving factors of its spatial differentiation in the northern foothills of the Yinshan Mountains in Inner Mongolia using Theil-Sen median slope analysis, the M − K test method and GeoDetector model. The NDVI in the northern foothills of the Yinshan Mountains has shown a significant increasing trend over the past 40 years, and vegetation cover in the study area has shown an overall increasing. The spatial distribution of NDVI was generally high in the east and low in the west. Future changes in vegetation NDVI are predicted to continue the 1982–2022 trend, sustainability improvements will continue to dominate in the future, however, there is still a potential risk that 17.69 % of the vegetation will continue to degrade or shift from improvement to degradation in the future. Climatic factors were the dominant drivers of NDVI spatial variability in the study area, and Pre had a greater effect than temperature on NDVI spatial patterns. Finally, the results of the risk detection analysis showed that each factor had the best range or characteristics for promoting vegetation growth, which can provide scientific references and decision-making bases for the development of grassland protection and management policies.

CRediT authorship contribution statement

Bo Yao: Writing – original draft, Visualization, Software, Data curation. **Xiangwen Gong:** Writing – review & editing, Formal analysis, Data curation, Conceptualization. **Yulin Li:** Supervision, Conceptualization. **Yuqiang Li:** Writing – review & editing, Funding acquisition. **Jie Lian:** Methodology, Formal analysis, Data curation. **Xuyang Wang:** Funding acquisition, Data curation, Conceptualization.

Data availability

Data will be made available on request.

Declaration of competing interest

The authors declare that the research was conducted in the absence of any commercial or financial relationships that could be construed as a potential conflict of interest.

Acknowledgments

This research was supported by the Yinshanbeilu Grassland Eco-hydrology National Observation and Research Station, China Institute of Water Resources and Hydropower Research, Beijing 100038, China, Grant NO. YS2022015; Youth Innovation Promotion Association of Chinese Academy of Sciences (2023449); Second Tibetan Plateau Scientific Expedition and Research (STEP) program (Grant No. 2019QZKK0305).

References

[1] L. Zhou, Y. Tian, R.B. Myneni, P. Ciais, S. Saatchi, Y.Y. Liu, S. Piao, H. Chen, E.F. Vermote, C. Song, T. Hwang, Widespread decline of Congo rainforest greenness in the past decade, Nature 509 (2014) 86–90, https://doi.org/10.1038/nature13265.

[2] G. Gutman, A. Ignatov, The derivation of the green vegetation fraction from NOAA/AVHRR data for use in numerical weather prediction models, Int. J. Rem. Sens. 19 (1998) 1533–1543, https://doi.org/10.1080/014311698215333.

[3] M. Gottfried, H. Pauli, A. Futschik, et al., Continent-wide response of mountain vegetation to climate change, Nat. Clim. Change 2 (2012) 111–115, https://doi.org/10.1038/nclimate1329.

[4] S. Huang, L. Tang, J.P. Hupy, Y. Wang, G. Shao, A commentary review on the use of normalized difference vegetation index (NDVI) in the era of popular remote sensing, J. For. Res. 32 (2021) 1–6, https://doi.org/10.1007/s11676-020-01155-1.

[5] K. Mo, Q. Chen, C. Chen, J. Zhang, L. Wang, Z. Bao, Spatiotemporal variation of correlation between vegetation cover and precipitation in an arid mountain-oasis river basin in northwest China, J. Hydrol. 574 (2019) 138–147, https://doi.org/10.1016/j.jhydrol.2019.04.044.

[6] I.A. Shah, Z. Muhammad, H. Khan, Impact of climate change on spatiotemporal variations in the vegetation cover and hydrology of district Nowshera, J. Water Clim. Change 13 (11) (2022) 3867–3882, https://doi.org/10.2166/wcc.2022.229.

[7] I.A. Shah, Z. Muhammad, H. Khan, R. Ullah, A. Rahman, Spatiotemporal variation in the vegetation cover of Peshawar Basin in response to climate change, Environ. Monit. Assess. 195 (2023) 1474, https://doi.org/10.1007/s10661-023-12094-9.

[8] I.A. Shah, H. Khan, Z. Muhammad, R. Ullah, S. Iqbal, H.-A. Nafidi, M. Bourhia, A.M. Salamatullah, Evaluation of climate change impact on plants and hydrology, Front. Environ. Sci. 12 (2024) 1328808, https://doi.org/10.3389/fenvs.2024.1328808.

[9] S. Shi, J. Yu, F. Wang, P. Wang, Y. Zhang, K. Jin, Quantitative contributions of climate change and human activities to vegetation changes over multiple time scales on the Loess Plateau, Sci. Total Environ. 755 (2021) 142419, https://doi.org/10.1016/j.scitotenv.2020.142419.

[10] W. Ge, L. Deng, F. Wang, J. Han, Quantifying the contributions of human activities and climate change to vegetation net primary productivity dynamics in China from 2001 to 2016, Sci. Total Environ. 773 (2021) 145648, https://doi.org/10.1016/j.scitotenv.2021.145648.

[11] X. Wang, S. Piao, P. Ciais, J. Li, P. Friedlingstein, C. Koven, A. Chen, Spring temperature change and its implication in the change of vegetation growth in North America from 1982 to 2006, Proc. Natl. Acad. Sci. U.S.A. 108 (4) (2011) 1240–1245, https://doi.org/10.1073/pnas.1014425108.

[12] W. Gao, C. Zheng, X. Liu, Y. Lu, Y. Chen, Y. Wei, Y. Ma, NDVI-based vegetation dynamics and their responses to climate change and human activities from 1982 to 2020: a case study in the Mu Us Sandy Land, China, Ecol. Indicat. 137 (2022) 108745, https://doi.org/10.1016/j.ecolind.2022.108745.

[13] X. Qi, J. Jia, H. Liu, Z. Liu, Relative importance of climate change and human activities for vegetation changes on China's silk road economic belt over multiple timescales, Catena 180 (2019) 224–237, https://doi.org/10.1016/j.catena.2019.04.027.

[14] H. Chu, S. Venevsky, C. Wu, M. Wang, NDVI-based vegetation dynamics and its response to climate changes at Amur-Heilongjiang River Basin from 1982 to 2015, Sci. Total Environ. 650 (2019) 2051–2062, https://doi.org/10.1016/j.scitotenv.2018.09.115.

[15] H. Liu, F. Jiao, J. Yin, T. Li, H. Gong, Z. Wang, Z. Lin, Nonlinear relationship of vegetation greening with nature and human factors and its forecast–A case study of Southwest China, Ecol. Indicat. 111 (2020) 106009, https://doi.org/10.1016/j.ecolind.2019.106009.

[16] X. Xu, H. Liu, F. Jiao, H. Gong, Z. Lin, Nonlinear relationship of greening and shifts from greening to browning in vegetation with nature and human factors along the Silk Road Economic Belt, Sci. Total Environ. 766 (2020) 142553, https://doi.org/10.1016/j.scitotenv.2020.142553.

[17] L. Yang, F. Shen, L. Zhang, Y. Cai, F. Yi, C. Zhou, Quantifying influences of natural and anthropogenic factors on vegetation change using structural equation modeling: a case study in Jiangsu Province. China, J. Clean. Prod. 280 (2021) 124330, https://doi.org/10.1016/j.jclepro.2020.124330.

[18] E. Ghaderpour, E.S. Ince, S.D. Pagiatakis, Least-squares cross-wavelet analysis and its applications in geophysical time series, J. Geodyn. 92 (2018) 1223–1236, https://doi.org/10.1007/s00190-018-1156-9.

[19] S. Huang, X. Zheng, L. Ma, H. Wang, Q. Huang, G. Leng, E. Meng, Y. Guo, Quantitative contribution of climate change and human activities to vegetation cover variations based on GA-SVM model, J. Hydrol. 584 (2020) 124687, https://doi.org/10.1016/j.jhydrol.2020.124687.

[20] J.F. Wang, T.L. Zhang, B.J. Fu, A measure of spatial stratified heterogeneity, Ecol. Indicat. 67 (2016) 250–256, https://doi.org/10.1016/j.ecolind.2016.02.052.

[21] H. Wang, F. Qin, C. Xu, B. Li, L. Guo, Z. Wang, Evaluating the suitability of urban development land with a GeoDetector, Ecol. Indicat. 123 (2021) 107339, https://doi.org/10.1016/j.ecolind.2021.107339.

[22] L.S. Zheng, Y.B. Li, Y. Chen, S.J. Yan, C.H. Xia, B. Zhang, J.A. Shao, Driving model of land use change on the evolution of carbon stock: a case study of Chongqing, China, Environ. Sci. Pollut. Res. 31 (2024) 4238–4255, https://doi.org/10.1007/s11356-023-31335-5.

[23] W.B. Zeng, X.M. Wan, G.Q. Gu, M. Lei, J. Yang, T.B. Chen, An interpolation method incorporating the pollution diffusion characteristics for soil heavy metals - taking a coke plant as an example, Sci. Total Environ. 857 (2023) 159698, https://doi.org/10.1016/j.scitotenv.2022.159698.

[24] L. Qu, H. Lu, Z. Tian, J.M. Schoorl, B. Huang, Y. Liang, D. Qiu, Y. Liang, Spatial prediction of soil sand content at various sampling density based on geostatistical and machine learning algorithms in plain areas, Catena 234 (2024) 107572, https://doi.org/10.1016/j.catena.2023.107572.

[25] F. Shen, C. Xu, J. Wang, M. Hu, G. Guo, T. Fang, X. Zhu, H. Cao, H. Tao, Y. Hou, A new method for spatial three-dimensional prediction of soil heavy metals contamination, Catena 235 (2024) 107658, https://doi.org/10.1016/j.catena.2023.107658.

[26] B. Yao, L. Ma, H. Si, S. Li, X. Gong, X. Wang, Spatial pattern of changing vegetation dynamics and its driving factors across the Yangtze River basin in Chongqing: a GeoDetector-based study, Land 12 (2023) 269, https://doi.org/10.3390/land12020269.

[27] H.Y. Zhao, X.H. Zhai, S. Li, Y.H. Wang, J.L. Xie, C.Z. Yan, The continuing decrease of sandy desert and sandy land in northern China in the latest 10 years, Ecol. Indicat. 154 (2023) 110699, https://doi.org/10.1016/j.ecolind.2023.110699.

[28] K. Wang, J. Zhou, M.L. Tan, P. Lu, Z. Xue, M. Liu, X. Wang, Impacts of vegetation restoration on soil erosion in the Yellow River Basin, China, Catena 234 (2024) 107547, https://doi.org/10.1016/j.catena.2023.107547.

[29] L. Kang, X. Han, Z. Zhang, O.J. Sun, Grassland ecosystems in China: review of current knowledge and research advancement, Philos. Trans. R. Soc. Lond. B Biol. Sci. 362 (2007) 997–1008, https://doi.org/10.1098/rstb.2007.2029.

[30] K. Zhang, H. Dang, S. Tan, X. Cheng, Q. Zhang, Change in soil organic carbon following the 'Grain-for-Green' programme in China, Land Degrad, Dev. 21 (2010) 13–23, https://doi.org/10.1002/ldr.954.

[31] P. Liang, X. Yang, Landscape spatial patterns in the Maowusu (Mu Us) Sandy Land, northern China and their impact factors, Catena 145 (2016) 321–333, https://doi.org/10.1016/j.catena.2016.06.023.

[32] Y. Zhao, D. Su, Y. Bao, W. Yang, C. Zhao, Y. Bai, Y. Zhao, Dynamic monitoring of fractional vegetation cover of eco-function area of grassland on northern foot of Yinshan Mountains through remote sensing technology, Res. Environ. Sci. 30 (2017) 240–248, https://doi.org/10.13198/j.issn.1001-6929.2017.01.35 (in Chinese).

[33] L. Zhang, Z. Ren, B. Chen, P. Gong, H. Fu, B. Xu, A Prolonged Artificial Nighttime-light Dataset of China (1984-2020), A Big Earth Data Platform for Three Poles, https://doi.org/10.11888/Socioeco.tpdc.271202.

[34] S. Li, L. Xu, Y. Jing, H. Yin, X. Li, X. Guan, High-quality vegetation index product generation: a review of NDVI time series reconstruction techniques, Int. J. Appl. Earth Obs. 105 (2021) 102640, https://doi.org/10.1016/j.jag.2021.102640.

[35] J.E. Pinzon, E.W. Pak, C.J. Tucker, U.S. Bhatt, G.V. Frost, M.J. Macander, Global Vegetation Greenness (NDVI) from AVHRR GIMMS-3G+, 1981-2022, ORNL DAAC, Oak Ridge, Tennessee, USA, 2023, https://doi.org/10.3334/ORNLDAAC/2187.

[36] C.J. Tucker, J.E. Pinzon, M.E. Brown, D.A. Slayback, E.W. Pak, R. Mahoney, E.F. Vermote, N.E. Saleous, An extended AVHRR 8 km NDVI dataset compatible with MODIS and SPOT vegetation NDVI data, Int. J. Rem. Sens. 26 (2005) 4485–4498, https://doi.org/10.1080/01431160500168686.

[37] F.H. Chen, B.J. Fu, J. Xia, D. Wu, S.H. Wu, Y.L. Zhang, et al., Major advances in studies of the physical geography and living environment of China during the past 70 years and future prospects, Sci. China Earth Sci. 49 (2019) 1659–1696, https://doi.org/10.1007/s11430-019-9522-7.

[38] J.E. Pinzon, C.J. Tucker, A non-stationary 1981-2012 AVHRR NDVI3g time series, Rem. Sens. 6 (2014) 6929–6960, https://doi.org/10.3390/rs6086929.

[39] A.F. Militino, M.D. Ugarte, U. Pérez-Goya, Stochastic spatio-temporal models for analysing NDVI distribution of GIMMS NDVI3g images, Rem. Sens. 9 (2017) 76, https://doi.org/10.3390/rs9010076.

[40] X.S. Zhang, Vegetation map of the People's Republic of China (1:1,000,000), Plant Data Center of Chinese Academy of Sciences, https://doi.org/10.12282/plantdata.0155.

[41] H.W. Mu, X.C. Li, Y.N. Wen, J.X. Huang, P.J. Du, W. Su, S.X. Miao, M.Q. Geng, A global record of annual terrestrial Human Footprint dataset from 2000 to 2018, Sci. Data 9 (2022) 176, https://doi.org/10.1038/s41597-022-01284-8.

[42] Y. Zhang, L.Q. Zhang, J.Y. Wang, G.C. Dong, Y.L. Wei, Quantitative analysis of NDVI driving factors based on the geographical detector model in the Chengdu-Chongqing region, China, Ecol. Indicat. 155 (2023) 110978, https://doi.org/10.1016/j.ecolind.2023.110978.

[43] J. Li, J.L. Wang, J. Zhang, C.L. Liu, S.L. He, L.F. Liu, Growing-season vegetation coverage patterns and driving factors in the China-Myanmar Economic Corridor based on Google Earth Engine and geographic detector, Ecol. Indicat. 136 (2022) 108620, https://doi.org/10.1016/j.ecolind.2022.108620.

[44] R. Fensholt, S.R. Proud, Evaluation of Earth Observation based global long term vegetation trends—comparing GIMMS and MODIS global NDVI time series, Remote Sens. Environ. 119 (2012) 131–147, https://doi.org/10.1016/j.rse.2011.12.015.
[45] H.B. Mann, Nonparametric tests against trend, Econometrica 13 (3) (1945) 245–259, 0012-9682(194507)13:3<245:NTAT>2.0.CO;2-U.
[46] M.G. Kendall, Kendall Rank Correlation Methods Griffin, 1975. London.
[47] K.H. Hamed, Trend detection in hydrologic data: the Mann–Kendall trend test under the scaling hypothesis, J. Hydrol. 349 (2008) 350–363, https://doi.org/10.1016/j.jhydrol.2007.11.009.
[48] H.E. Hurst, Long-term storage capacity of reservoirs, Trans. Am. Soc. Civ. Eng. 116 (1951) 770–799.
[49] Z. Sánche, J.E. Trinidad, P.J. García, Some comments on Hurst exponent and the long memory processes on capital markets, Physica A 387 (2008) 5543–5551, https://doi.org/10.1016/j.physa.2008.05.053.
[50] B.B. Mandelbrot, J.R. Wallis, Robustness of the rescaled range R/S in the measurement of noncyclic long run statistical dependence, Water Resour. Res. 5 (1969) 967–988, https://doi.org/10.1029/WR005i005p00967.
[51] X. Zeng, Z. Hu, A. Chen, W. Yuan, G. Hou, D. Han, M. Liang, K. Di, R. Cao, D. Luo, The global decline in the sensitivity of vegetation productivity to precipitation from 2001 to 2018, Global Change Biol. 28 (2022) 6823–6833, https://doi.org/10.1111/gcb.16403.
[52] S. Wang, R. Li, Y. Wu, S. Zhao, Effects of multi-temporal scale drought on vegetation dynamics in Inner Mongolia from 1982 to 2015, China, Ecol. Indicat. 136 (2022) 108666, https://doi.org/10.1016/j.ecolind.2022.108666.
[53] B. Gao, X. Ye, L. Ding, P. Zhang, Y. Wang, L. Xiao, Water availability dominated vegetation productivity of Inner Mongolia grasslands from 1982 to 2015, Ecol. Indicat. 151 (2023) 110291, https://doi.org/10.1016/j.ecolind.2023.110291.
[54] S. Wang, Y. Zhang, W. Ju, J.M. Chen, P. Ciais, A. Cescatti, J. Sardans, I.A. Janssens, M. Wu, J.A. Berry, E. Campbell, M. Fernández-Martínez, R. Alkama, S. Sitch, P. Friedlingstein, W.K. Smith, W. Yuan, H. He, D. Lombardozzi, M. Kautz, D. Zhu, S. Lienert, E. Kato, B. Poulter, T.G.M. Sanders, I. Krüger, R. Wang, N. Zeng, H. Tian, N. Vuichard, A.K. Jain, A. Wiltshire, V. Haverd, D.S. Goll, J. Peñuelas, Recent global decline of CO2 fertilization effects on vegetation photosynthesis, Science 370 (2020) 1295–1300, https://doi.org/10.1126/science.abb7772.
[55] C. Dong, X. Wang, Y. Ran, Z. Nawaz, Heatwaves significantly slow the vegetation growth rate on the Tibetan Plateau, Rem. Sens. 14 (2022) 2402, https://doi.org/10.3390/rs14102402.
[56] J. Huang, Y. Xue, S. Sun, J. Zhang, Spatial and temporal variability of drought during 1960–2012 in Inner Mongolia, north China, Quat. Int. 355 (2015) 134–144, https://doi.org/10.1016/j.quaint.2014.10.036.
[57] G.A. Afuye, A.M. Kalumba, I.R. Orimoloye, Characterisation of vegetation response to climate change: a review, Sustainability 13 (2021) 7265, https://doi.org/10.3390/su13137265.
[58] L. He, J. Guo, W. Yang, Q. Jiang, L. Chen, K. Tang, Multifaceted responses of vegetation to average and extreme climate change over global drylands, Sci. Total Environ. 858 (2022) 159942, https://doi.org/10.1016/j.scitotenv.2022.159942.
[59] H.J. Tian, C.X. Cao, W. Chen, S.N. Bao, B. Yang, R.B. Myneni, Response of vegetation activity dynamics to climatic change and ecological restoration programs in Inner Mongolia from 2000 to 2012, Ecol. Eng. 82 (2015) 276–289, https://doi.org/10.1016/j.ecoleng.2015.04.098.
[60] W. Fang, S. Huang, Q. Huang, G. Huang, H. Wang, G. Leng, L. Wang, P. Li, L. Ma, Bivariate probabilistic quantification of drought impacts on terrestrial vegetation dynamics in mainland China, J. Hydrol. 577 (2019) 123980, https://doi.org/10.1016/j.jhydrol.2019.123980.
[61] Z. Shen, Q. Zhang, V.P. Singh, P. Sun, C. Song, H. Yu, Agricultural drought monitoring across Inner Mongolia, China: model development, spatiotemporal patterns, and impacts, J. Hydrol. 571 (2019) 793–804, https://doi.org/10.1016/j.jhydrol.2019.02.028.
[62] Y. Wang, G. Liu, E. Guo, Spatial distribution and temporal variation of drought in inner Mongolia during 1901–2014 using standardized precipitation evapotranspiration index, Sci. Total Environ. 654 (2019) 850–862, https://doi.org/10.1016/j.scitotenv.2018.10.425.
[63] Q. Guo, Z. Hu, S. Li, X. Li, X. Sun, G. Yu, Spatial variations in aboveground net primary productivity along a climate gradient in Eurasian temperate grassland: effects of mean annual precipitation and its seasonal distribution, Global Change Biol. 18 (2012) 3624–3631, https://doi.org/10.1111/gcb.12010.
[64] Z. Hu, Q. Guo, S. Li, S. Piao, A.K. Knapp, P. Ciais, X. Li, G. Yu, J. Knops, Shifts in the dynamics of productivity signal ecosystem state transitions at the biome-scale, Ecol. Lett. 21 (2018) 1457–1466, https://doi.org/10.1111/ele.13126.
[65] R. Su, T. Yu, B. Dayananda, R. Bu, J. Su, Q. Fan, Impact of climate change on primary production of Inner Mongolian grasslands, Glob. Ecol. Conserv. 22 (2020) e00928, https://doi.org/10.1016/j.gecco.2020.e00928.
[66] Z. Hu, M. Liang, A. Knapp, J. Xia, W. Yuan, Are regional precipitation-productivity relationships robust to decadal-scale dry period? J. Plant Ecol. 15 (2022) 711–720, https://doi.org/10.1093/jpe/rtac008.
[67] A. Zhao, Q. Yu, L. Feng, A. Zhang, T. Pei, Evaluating the cumulative and time-lag effects of drought on grassland vegetation: a case study in the Chinese Loess Plateau, J. Environ. Manag. 261 (2020) 110214, https://doi.org/10.1016/j.jenvman.2020.110214.
[68] R.R. Nemani, C.D. Keeling, H. Hashimoto, W.M. Jolly, S.C. Piper, C.J. Tucker, R.B. Myneni, S.W. Running, Climate-driven increases in global terrestrial net primary production from 1982 to 1999, Science 300 (5625) (2003) 1560–1563, https://doi.org/10.1126/science.1082750.
[69] T. Hua, X. Wang, Temporal and spatial variations in the climate controls of vegetation dynamics on the Tibetan plateau during 1982–2011, Adv. Atmos. Sci. 35 (2018) 1337–1346, https://doi.org/10.1007/s00376-018-7064-3.
[70] D. Liu, T. Wang, T. Yang, Z. Yan, Y. Liu, Y. Zhao, S. Piao, Deciphering impacts of climate extremes on Tibetan grasslands in the last fifteen years, Sci. Bull. 64 (7) (2019) 446–454, https://doi.org/10.1016/j.scib.2019.03.012.
[71] J.Y. Wang, Y.J. Liu, Y.R. Li, Ecological restoration under rural restructuring: a case study of Yan'an in China's loess plateau, Land Use Pol. 87 (2019) 104087, https://doi.org/10.1016/j.landusepol.2019.104087.
[72] M.B. Dodd, W.K. Lauenroth, I.C. Burke, P.L. Chapman, Associations between vegetation patterns and soil texture in the shortgrass steppe, Plant Ecol. 158 (2002) 127–137, https://doi.org/10.1023/A:1015525303754.
[73] M.A. Sanderson, M.A. Liebig, J.R. Hendrickson, S.L. Kronberg, D. Toledo, J.D. Derner, J.L. Reeves, Long-term agroecosystem research on northern Great Plains mixed-grass prairie near Mandan, North Dakota, Can, J. Plant Sci. 95 (6) (2015) 1101–1116, https://doi.org/10.4141/CJPS-2015-117.
[74] P. Jiang, W. Ding, Y.e. Yuan, W. Ye, Diverse response of vegetation growth to multi-time-scale drought under different soil textures in China's pastoral areas, J. Environ. Manag. 274 (2020) 110992, https://doi.org/10.1016/j.jenvman.2020.110992.
[75] E.A. Petropoulos, P.S. Timiras, Biological effects of high altitude as related to increased solar radiation, temperature fluctuations and reduced partial pressure of oxygen, Prog. Biometeorol. 1 (1A) (1974) 295–328.
[76] L. Liu, X. Yang, H. Zhou, S. Liu, L. Zhou, X. Li, J. Yang, J. Wu, Relationship of root zone soil moisture with solar-induced chlorophyll fluorescence and vegetation indices in winter wheat: a comparative study based on continuous ground-measurements, Ecol. Indicat. 90 (2018) 9–17, https://doi.org/10.1016/j.ecolind.2018.02.048.